Archives of Biochemistry and Biophysics 528 (2012) 7–20

Contents lists available at SciVerse ScienceDirect

Archives of Biochemistry and Biophysics

journal homepage: www.elsevier.com/locate/yabbi

A role for His-160 in peroxide inhibition of *S. cerevisiae* *S*-formylglutathione hydrolase: Evidence for an oxidation sensitive motif

Patricia M. Legler [a,*], Dagmar H. Leary [a], William Judson Hervey IV [a], Charles B. Millard [b]

[a] *Center of Bio/Molecular Science and Engineering, Naval Research Laboratories, Washington, DC 20375, USA*
[b] *U.S. Army Medical Research & Materiel Command, Frederick, MD 21702-5012, USA*

ARTICLE INFO

Article history:
Received 22 May 2012
and in revised form 31 July 2012
Available online 13 August 2012

Keywords:
Organophosphate
Sulfenic acid
Sulfinic acid
Sulfonic acid
Oxidation
Motif
Glutathione
Serine hydrolase
Carboxylesterase
Thioesterase

ABSTRACT

While the general catalytic mechanism of the widespread serine hydrolase superfamily has been documented extensively, much less is known about its varied modes of functional modulation within biological systems. Under oxidizing conditions, inhibition of *Saccharomyces cerevisiae* *S*-formylglutathione hydrolase (SFGH, homologous to human esterase D) activity is attributable to a cysteine (Cys-60) adjacent to its catalytic triad and approximately 8.0 Å away from the Oγ of the nucleophilic serine. Cys-60 is oxidized to a sulfenic acid in the structure of the Paraoxon-inhibited W197I variant (PDB 3C6B). The structural snap-shot captured an unstable reversibly oxidized state, but it remained unclear as to whether the oxidation occurred before, during, or after the reaction with the organophosphate inhibitor. To determine if the oxidation of Cys-60 was functionally linked to ester hydrolysis, we used kinetic analysis and site-directed mutagenesis in combination with X-ray crystallography. The essential nature of Cys-60 for oxidation is demonstrated by the C60S variant, which is not inhibited by peroxide in the presence or absence of substrate. In the presence of substrate, the rate of inhibition of the WT SFGH by peroxide increases 14-fold, suggesting uncompetitive behavior linking oxidation to ester hydrolysis. Here we found one variant, H160I, which is activated by peroxide. This variant is activated at comparable rates in the presence or absence of substrate, indicating that the conserved His-160 is involved in the inhibitory mechanism linking ester hydrolysis to the oxidation of Cys-60. Copper chloride inhibition experiments show that at least two metal ions bind and inhibit both WT and H160I. A structure of the Paraoxon-inhibited W197I variant soaked with $CuCl_2$ shows density for one metal ion per monomer at the N-terminus, and density around the Cys-60 sulfur consistent with a sulfinic acid, Cys-SO_2. A Dali structural similarity search uncovered two other enzymes (*Bacillus subtilis* RsbQ, 1WOM and *Clostridium acetobutylicum* Lipase–esterase, 3E0X) that contain a similar Cys adjacent to a catalytic triad. We speculate that the regulatory motif uncovered is conserved in some D-type esterases and discuss its structural similarities in the active site of human protective protein (HPP; also known as Cathepsin A).

Published by Elsevier Inc.

Serine hydrolases are widespread, comprising as much as 1% of the human proteome, and the canonical catalytic triad (or dyad) and "oxyanion hole" motifs of this superfamily are among the most intensely studied and well documented of all enzyme active sites. However, remarkably little is known of the general mechanisms by which catalysis by these enzymes can be controlled or modulated to achieve desired biological functions. D-type esterases are a group of serine hydrolases that were first characterized by their resistance to organophosphate inhibition and susceptibility to inhibition by *N*-ethylmaleimide (NEM)[1], copper and mercury [1]. While characterizing the mechanism of organophosphate resistance in a D-type esterase, *Saccharomyces cerevisiae* *S*-formylglutathione hydrolase (SFGH, EC 3.1.2.12), we trapped a cysteine sulfenic acid

* Corresponding author. Address: Naval Research Laboratories, 4555 Overlook Ave., Washington, DC 20375, USA.
E-mail address: plegler2@gmail.com (P.M. Legler).

[1] *Abbreviations used:* bME, beta-mercaptoethanol; CD, circular dichroism; CE, carboxylesterase; DEP, diethyl phosphate; DMSO, dimethylsulfoxide; DTT, dithiothreitol; EDTA, ethylenediaminetetraacetic acid; ESI-MS, electrospray ionization-mass spectrometry; FA, formic acid; hEstD, human esterase-D; HPP, human protective protein/Cathepsin A; MALDI-TOF, matrix assisted laser desorption ionization-time of flight mass spectrometry; NanoLC–MS/MS, nanoflow liquid chromatography electrospray ionization tandem mass spectrometry; NBD chloride, 7-chloro-4-nitrobenzo-2-oxa-1,3-diazole; NEM, *N*-ethylmaleimide; OP, organophosphate; Paraoxon, diethyl 4-nitrophenyl phosphate; pNPA, *p*-nitrophenyl acetate; Rsb, regulator of sigma b; R.T., room temperature; SDS–PAGE, sodium dodecylsulfate–polyacrylamide gel electrophoresis; SFGH, *S*-formylglutathione hydrolase; SLG, *S*-lactoylglutathione; TS, transition state; WT, wild type; y, yeast.

0003-9861/$ - see front matter Published by Elsevier Inc.
http://dx.doi.org/10.1016/j.abb.2012.08.001

[2]. Here we show that the loss of esterase activity in the presence of copper or peroxide is due to a cysteine (Cys-60) adjacent to its catalytic triad and that the loss of esterase activity upon oxidation of this cysteine involves His-160.

Growing interest in the functional role of cysteine-sulfenic acids has arisen over the past 10 years [3] due to the advent of sulfenic-acid-specific reagents, such as dimedone and NBD-chloride [3,4], and their use in proteomic studies [5]. Peroxide can be generated during oxidative metabolism, but also by ionizing radiation. The molecular mechanisms by which reactive oxygen species exert their effects on specific enzymes is less well understood, as are oxidation-susceptible motifs which can control enzyme activity. The sulfenic acid (R-SOH) is of particular interest because the relatively unstable oxidized state can be readily reversed by reaction with a free thiol unlike the sulfinic ($R\text{-}SO_2H$) and sulfonic acids ($R\text{-}SO_3H$). Reaction of a sulfenic acid (R-SOH) with a free thiol (R-SH) results in the loss of water and formation of a disulfide.

$$R\text{-}SOH + R' - SH \rightarrow R\text{-}S\text{-}S\text{-}R' + H_2O \quad (1)$$

SFGH catalyzes the hydrolysis of *S*-formylglutathione and produces formate and glutathione. Glutathione produced from the SFGH-catalyzed reaction may play an important role in the reversible oxidation of the esterase as the glutathionylated enzyme has been identified in mass spectra [6].

The instability of sulfenic acids has made them difficult to characterize except in cases where the sulfenic acid can be trapped or stabilized by residues surrounding the modification. Paraoxon inhibition resulted in the trapping of a sulfenic acid in the structure of the Paraoxon-inhibited W197I SFGH variant (PDB 3C6B) (Fig. 1A). The oxidation of cysteines has been generally linked to the inhibition of catalysis (e.g. protein tyrosine phosphatases [7,8], glutathione reductase [9], superoxide dismutase [10]). However, the oxidation of a cysteine does not demonstrate a functional role for a sulfenic acid in the regulation of an enzyme as some cysteines are susceptible to this form of oxidation for other reasons. In addition, cysteine oxidation, as we show here, is not necessarily inhibitory. Based upon the X-ray structure alone it was not possible to determine if the hydrolysis reaction was linked to the oxidation of the cysteine as Paraoxon inhibition, or rather occupancy of the oxyanion hole, could alter the pK_a of the adjacent cysteine and make it more susceptible to oxidation. To show that the oxidation of the cysteine could affect the esterase activity, we used site-directed mutagenesis and examined the effects of peroxide on the activity of WT SFGH and its variants. Unexpectedly, one variant, H160I, was found to be activated by peroxide.

Materials and methods

Materials

BugBuster™ was from Novagen (San Diego, CA). Q-Sepharose and PD-10 columns were from GE Healthcare Life Sciences (Piscataway, NJ). C18 ZipTips were from Millipore (Billerica, MA). QuikChange™ kits were purchased from Stratagene (La Jolla, CA). A stabilized solution of peroxide, Perdrogen®, was used for all oxidation experiments. Bio-Spin 6 gel filtration columns were purchased from BioRad (Hercules, CA). G-25 and G-75 Sephadex, catalase from bovine liver and all substrates and inhibitors were purchased from Sigma.

Protein expression and purification

Detailed procedures for the expression and purification of SFGH and its mutants have been published [2]. SFGH and its variants were purified to ⩾95% purity (based upon SDS–PAGE) without affinity tags or any other modifications. Protein concentrations were determined from the absorbance at 280 nm using a molar extinction coefficient of 56.1 $mM^{-1}\,cm^{-1}$.

Carboxylesterase assays

Steady state kinetic parameters were measured at room temperature in 1× Sorensen's buffer (53.4 mM Na_2HPO_4, 13.4 mM KH_2PO_4) pH 7.4. Enzymes were diluted in 1× Sorensen's buffer containing 2 mM beta-mercaptoethanol (bME). Substrate and inhibitors were dissolved in DMSO and comprised no more than 1% of the reaction volume. A Unit was defined as μmol product produced per minute.

Copper inhibition kinetics

A 1 × 25 cm G-25 Sephadex column was necessary (50 mM HEPES pH 7.0 and 150 mM NaCl) to remove any bME and/or EDTA that was present in the storage buffer. Since copper can catalyze the oxidation of cysteines to sulfenic acids with peroxide or superoxide, enzyme solutions were added immediately to assay solutions containing buffer, substrate and copper before measurements (30 s reads) of the absorbance to prevent copper catalyzed oxidation of the cysteine. The V_{max} and $K_{m,apparent}$ were measured in the absence and in the presence of $CuCl_2$ at R.T. (22 ± 2 °C) in 50 mM HEPES pH 7.0, 150 mM NaCl. Concentrations of $CuCl_2$ greater than 30 μM precipitated in the buffer. Six different concentrations of pNPA were used at each inhibitor concentration and data were globally fit using Grafit 3.0 (Erithacus Software Ltd.).

Rates of inactivation or activation by hydrogen peroxide in the absence of substrate

Enzyme solutions were pretreated with 20 mM DTT for at least 5 min. The reducing agent was removed by a gel filtration (a G-25 Sephadex column or a PD-10) column equilibrated with 1× Sorensen's buffer pH 7.4. Inactivation rates at varying concentrations of peroxide were measured for the WT SFGH in the absence of substrate at R.T. Aliquots were removed and assayed over time (15–30 s) in 1× Sorensen's buffer, pH 7.4 containing 857 Units of bovine liver catalase (to remove peroxide from assay mixtures) and 5 mM pNPA. Rates were also measured in the absence of catalase. Data were fit to Eq. 3 [11].

$$HOOH + E\text{-}SH \overset{K_i}{\Longleftrightarrow} E - SH \cdot HOOH \overset{k_2}{\rightarrow} E\text{-}SOH + H_2O \quad (2)$$

$$k_{obs} = \frac{k_2}{1 + K_i/[I]} \quad (3)$$

where k_2 is the first-order rate constant for inactivation (or activation), K_i (or K_a), is the dissociation constant of peroxide from the E-SH·HOOH complex and k_{obs} is the apparent first-order rate constant of inactivation (or activation) measured for each peroxide concentration.

Rate of inactivation or activation by hydrogen peroxide in the presence of substrate

Enzyme solutions (0.006–0.016 mM) were treated with an excess of peroxide in the presence of a saturating concentration of substrate, 5 mM pNP-acetate, or as a control, 5 mM *p*-nitrophenol. The pNPA was added to the enzyme and incubated at room temperature for 1 min prior to the addition of peroxide. Aliquots were removed and assayed over time in 1× Sorensen's buffer, pH 7.4 containing 857 Units of bovine liver catalase and 5 mM pNP-acetate. The concentrations of peroxide were measured using an extinction coefficient of 43.6 $M^{-1}\,cm^{-1}$ at 240 nm. Data were fit to Eq. 3.

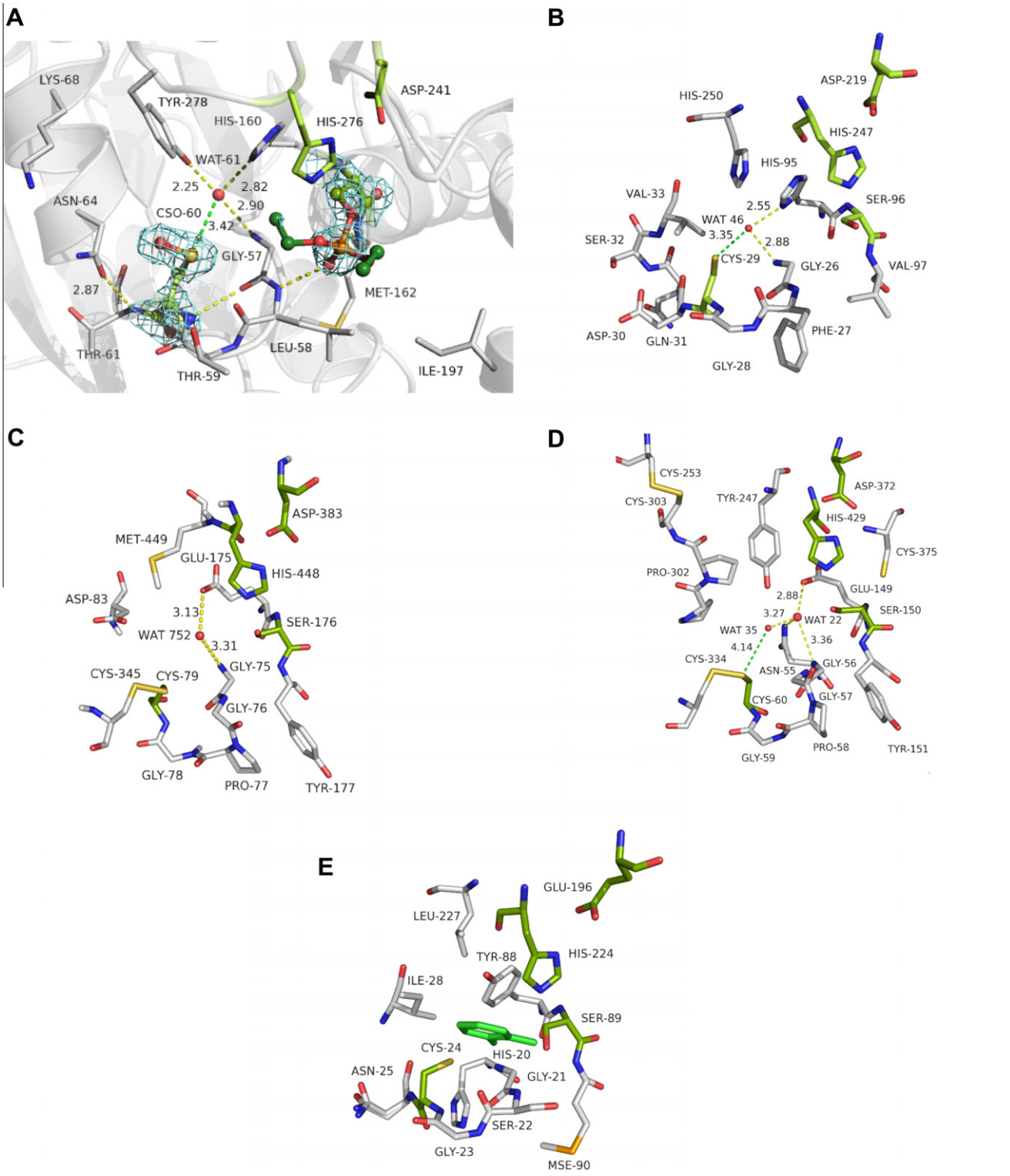

Fig. 1. Comparison of four structurally similar enzymes. (A) The W197I variant of *S. cerevisiae* SFGH (PDB 3C6B) inhibited with Paraoxon. The catalytic triad (shown in lime) is formed by Ser-161/His-276/Asp-241. (B) *Bacillus subtilis* RsbQ (PDB 1WOM). The catalytic triad is formed by Ser-96/His-247/Asp-219. (C) *S. cerevisiae* killer factor and prohormone-processing carboxypeptidase, Kex1ΔP (PDB 1AC5). The catalytic triad is formed by Ser-176/His-448/Asp-383. Kex1ΔP is the yeast homologue of the enzyme shown in D. (D) Human protective protein/Cathepsin A (PDB 1IVY). The catalytic triad is formed by Ser-150/His-429/Asp-372. (E) *Clostridium acetobutylicum* Lipase–esterase (PDB 3E0X). The catalytic triad is formed by Ser-89/His-224/Glu-196. Figure was prepared using Pymol (DeLano Scientific).

For the H160I variant, the enzyme was incubated at R.T. for 1 min with 5 mM pNP-acetate and then treated with 3.3 mM peroxide. After 25 min the treated enzyme was loaded onto a PD-10 gel filtration column and the fraction containing H160I was diluted and then assayed 12, 45 and 60 min after treatment with peroxide using pNP-acetate as the substrate. An aliquot of the eluted enzyme was treated with catalase (8568 U) for 12 min prior to activity assays.

Thiol titrations

To measure the number of accessible thiol groups in the native enzyme, protein was pre-treated with 20 mM DTT and then desalted using PD-10 columns equilibrated with 1× Sorensen buffer pH 7.4. Protein (2–11 μM) was aliquoted into microcentrifuge tubes. Denatured samples were boiled for 2.5 min at 100 °C. Tubes were then chilled in an ice bath for 5 min to prevent hydrolysis of DTNB. Volumes were adjusted to 1.0 mL with 1× Sorensen's buffer pH 7.4 and DTNB (0.5 mM final concentration of DTNB). Reactions were incubated in the dark for 25 min and the precipitate was removed by centrifugation (10,000 rpm, 2 min). The absorbance at 412 nm was measured and the concentration of 5-thio-2-nitrobenzoic acid was determined using an extinction coefficient of 13.6 mM^{-1} cm^{-1} [12]. At least three concentrations of enzyme were used for each determination. The moles of enzyme were plotted against moles of 5-thio-2-nitro-benzoic acid and the number of titratable thiols was determined from the slope of the line. A solution of glutathione was used as a control.

Circular dichroism

Thermal denaturation of the WT and variants was monitored from 45 to 80 °C (2 °C per minute) using a Jasco 810 Circular Dichroism spectropolarimeter fitted with a Peltier temperature controller. Protein was exchanged into 1× Sorensen pH 7.4, 2 mM beta mercaptoethanol. The apparent melting temperature was determined from a four parameter fit of the averaged ellipticity (mdeg) at 222 nm versus temperature from at least two variable temperature scans at the same protein concentration.

NBD-chloride assays

WT SFGH containing 20 mM DTT was buffer exchanged into 1× Sorensen's buffer using a PD-10 column. The enzyme (0.024 mM) was reacted with substrate (5 mM pNPA) for 1 min and inhibited with peroxide (3.8 mM) for 17 min at room temperature. NBD-chloride in DMSO (17 mM final concentration) was added and reacted for approximately 50 min at room temperature and stored at 4 °C in the dark overnight. Unreacted NBD-chloride was removed by a Bio-Spin 6 column equilibrated with 1× Sorensen pH 7.4. The modified protein was buffer exchanged four times using an ultrafiltration unit (10,000 MWCO). UV–vis spectra were collected for the modified protein and the flow through to verify that the spectra was of the modified protein.

pH-rate profile

The pH dependence of NEM inhibition was measured in 0.2 M sodium phosphate buffer and 22 °C at each pH. NEM was dissolved in ethanol and at least four concentrations of NEM were used to calculate k_2 and K_i using Eq. 3. The concentration of ethanol was held constant at 3.3%. Activity was measured using pNP-acetate in 0.2 M sodium phosphate buffer at each pH. The bell-shaped pH-rate profiles were fit using Eq. 4 and the Grafit software package, where k_2/K_i(limit) is the pH-independent maximum rate constant.

$$\frac{k_2}{K_i} = k_2/K_i(\text{limit})\left(\frac{1}{1+10^{pK_1-\text{pH}}+10^{\text{pH}-pK_2}}\right) \quad (4)$$

MALDI-TOF mass spectrometry

Wild type SFGH was inhibited with peroxide (3.8 mM) in the presence of pNP-acetate (5 mM) at room temperature. After 20 min of inhibition the enzyme was loaded onto a PD-10 gel filtration column (equilibrated with 200 mM Ammonium Bicarbonate pH 8.0) to remove the peroxide, substrate and product. The protein was then digested with trypsin at room temperature for 48 h. Zip-tips (C18) were wetted with 50% acetonitrile (ACN)/H_2O. Tips were then equilibrated with 0.1% trifluoroacetic acid (TFA) in water, loaded with sample and washed again in the same solution. Tips were eluted with 0.1% TFA/50% ACN and the eluate was spotted onto the target with dihydroxybenzoic acid (dissolved in 50% ACN and water) using the method of Onnerfjord et al. [13]. Spectra were collected on a Shimadzu Biotech Axima CFRplus mass spectrometer in linear negative mode and positive reflectron mode to identify the Cys60-SO_3 and Cys60-SO_2 species.

Liquid chromatography nano-electrospray ionization tandem mass spectrometry (nanoLC–MS/MS)

To identify modifications of the treated and untreated H160I variants, two separate types of nanoLC–MS/MS experiments were used to characterize proteolytic peptides produced from protease digestions in an organic-aqueous (acetonitrile–water) solvent, as described previously [14]. First, preliminary experiments to characterize putative modification sites of each variant were performed, followed by a series of targeted product ion scans to pinpoint modification site(s) in tandem mass spectra. Mass spectrometry data were acquired on a QSTAR Elite quadrupole time of flight mass spectrometer coupled to a one-dimensional reverse-phase HPLC system via a nanoelectrospray III source (AB Sciex, Foster City, CA) operated under control of the AnalystQS software. Product ion spectra of precursor ions corresponding to endoproteinase LysC proteolytic peptides with trioxidation (787.393+) and dioxidation (782.073+) of Cys-60 were acquired throughout the LC gradient. Tandem mass spectra (MS/MS) corresponding to the peptide sequence containing Cys-60 (RIPTVFYLSGLTCTPDNASEK) were detected at a retention time of 28 min (for both modifications), with peak width of ~1 min. Average MS/MS spectra of the modifications were extracted and annotated. Further description of the nanoLC–MS/MS workflow performed is provided in the accompanying Supplemental information.

Crystallization and structure determination of the H160I variant and the W197I variant with copper and diethylphosphate

The W197I variant was crystallized in Hampton Crystal Screen Cryo solution number 10 (0.17 M Ammonium acetate, 0.085 M sodium acetate trihydrate pH 4.6, 25.5% PEG 4000, 15% glycerol). Protein was prepared as described previously [2]. Crystals were soaked with 23 mM ethyl paraoxon for 7 days. Copper chloride (2.4 mM final concentration) was added and crystals were flash frozen in liquid nitrogen after 7 min of soaking. Data were collected at 100 K using a Bruker FR591 high-flux, rotating anode X-ray diffractometer (PROTEUM) and a SMART 6000 2 K CCD detector. Initial phases were calculated from PDB 3C6B, and the structure was determined by molecular replacement using Amore [15]. CNS was used for simulated annealing. The model was refined using Refmac 5 [16,17] and Coot [18].

The H160I variant was crystallized in the same precipitant. Crystals were drawn through Paratone-N and flash frozen in liquid nitrogen. The structure was also determined by molecular replacement and refined using Refmac 5.

Results

Thiol titrations

SFGH contains five cysteines. In the structure of the WT enzyme (PDB 1PV1) [2] there are no disulfide bonds. In the heat denatured

protein all five cysteines could be titrated by Ellman's reagent, whereas, only one cysteine was titratable in the native protein. To verify that the titratable cysteine was Cys-60 in the native enzyme we titrated the C60S variant. With the native C60S variant no titratable cysteines were detected while all four cysteines could be detected in the denatured C60S variant (Table 1). Thus, only Cys-60 is accessible to DTNB and solvent in the native state. Cys-60 was found as a sulfenic acid in the structure of the Paraoxon-inhibited W197I variant. Titration of WT SFGH with DTNB in the absence of substrate or inhibitor yielded a stoichiometry near one (1.07 ± 0.08) indicating that the thiol of Cys-60 is in the reduced state.

Steady state kinetic parameters of WT SFGH and the C60A and C60S variants

Steady state kinetic parameters were previously determined for the WT, W197I and C60S variants using pNP-acetate as the substrate (Table 2) [2]. Mutation of Cys-60 to serine or alanine (C60A) has only a minor effect (less than 2-fold) on K_m and on k_{cat} for pNP-acetate hydrolysis indicating that Cys-60 is dispensable for esterase activity.

Previously, we showed that expansion of the acyl pocket by mutation of W197 to Ile enabled hydrolysis of a commercially available *S*-lactoylglutathione substrate. The substrate contains an additional $-CH(OH)CH_3$ group when compared to the *S*-formylglutathione (SFG) substrate (*n.b.* SFG undergoes rapid spontaneous hydrolysis in <30 s in water). The C60S mutation did not significantly affect hydrolysis of an *S*-lactoylglutathione substrate (Table 2) suggesting no significant role for this residue in substrate binding or catalysis.

Inhibition of WT and C60S SFGH activity by peroxide in the presence or absence of substrate

To determine if the oxidation of Cys-60 is coupled to the hydrolysis of the ester, the rate of inactivation by peroxide was initially measured in the presence of substrate (5 mM pNPA) with a single concentration of peroxide (3.6 mM) and compared to the rate measured in the absence of substrate (Fig. 2A and Table 3). The rate of inactivation by peroxide (k_{obs}) increased 26-fold in the presence of the substrate. As a control, the reaction was run in the presence of an equal concentration of *p*-nitrophenol and no additional effect was observed; the rates of inactivation by peroxide in the presence or absence of added *p*-nitrophenol were comparable.

The C60S variant was not inactivated by peroxide (7–70 mM) supporting the involvement of Cys-60 in oxidative inactivation. With 3.6 mM peroxide, the C60S variant remained uninhibited in the presence or absence of substrate (Fig. 2B) demonstrating a clear requirement for Cys-60 in the peroxide inhibition mechanism.

Maximum rates of inactivation were then measured using the method of Kitz and Wilson [11] with varying concentrations of peroxide in the presence or absence of substrate (5 mM pNPA) (Table 4 and Fig. 2C). Aliquots of the enzyme, enzyme/peroxide, or enzyme/pNP-acetate/peroxide solution were removed and assayed over time.

Table 1
Thiol titrations of native and denatured WT SFGH and the C60S variant.

Enzyme	State	Number of cysteines (Slope)	Intercept
WT	Native	1.07 ± 0.08	−0.0003 ± 0.0003
WT	Denatured	4.9 ± 0.3	−0.001 ± 0.003
C60S	Native	0.1 ± 0.2	−0.001 ± 0.001
C60S	Denatured	4.02 ± 0.08	0.0003 ± 0.0006

The WT enzyme could be inactivated by hydrogen peroxide with a maximum rate constant of 0.116 ± 0.005 min^{-1} with a K_i = 12 ± 3 mM (catalase was present in the assay mix). Catalase was added to prevent further oxidation during the measurement period, but was found to be unnecessary. When the pNP-acetate substrate was first added to the enzyme prior to peroxide a faster rate of inactivation was observed. In the presence of substrate (5 mM pNPA), the rate constant of inactivation was 10-fold faster (k_2 = 1.0 ± 0.5 min^{-1}, K_i = 8 ± 5 mM) than in the absence of substrate suggesting uncompetitive behavior (i.e. formation of an E–S–I complex).

The sulfenic acid at Cys-60 was initially trapped in the crystalline state upon inhibition with Paraoxon, a suicide inhibitor and tetrahedral transition state mimic, which forms a covalent adduct with the nucleophilic Ser-161. NBD-chloride was used to verify the formation of a sulfenic acid in solution in the presence of a substrate (pNP-acetate) and peroxide. A maxima at 347 nm corresponding to an NBD chloride–sulfenic acid (Cys-SOH) adduct and a maxima at 420 nm corresponding to a thiol adduct of NBD-chloride (Cys-SH) (4) were observed when the WT enzyme was treated with peroxide in the presence of substrate followed by treatment with NBD-chloride (Supplemental Fig. 1). The presence of the 347 nm peak demonstrated that the R-SOH species is formed in solution when the hydrolysis of the substrate is catalyzed.

Mass spectrometric detection of the Cys-SO_2 and Cys-SO_3 species

The sulfenic acid was initially trapped in SFGH using diethylphosphate where only a single turnover can occur. To determine if multiple rounds of oxidation could occur at Cys-60 during substrate hydrolysis mass spectrometry was used to detect the Cys-SO_2 and Cys-SO_3 species. The oxidized cysteines were observed in linear negative mode for the WT SFGH (Supplemental Table 1) using MALDI-TOF MS. The presence of the Cys-SO_3 species and to a smaller degree, the Cys-SO_2 species, demonstrates that the Cys-SOH species can be further oxidized to the sulfinic and sulfonic acids when substrate (pNP-acetate) and peroxide are present. Oxidation of Cys-60 in the H160I variant was not initially observed by MALDI-TOF, however the modification was observed using electrospray nanoLC–MS/MS (Fig. 3). The sequenced peptides indicate that the Cys-60 of the H160I variant can also be oxidized to the Cys-SO_2 and Cys-SO_3 states. It is important to note that in the crystal structure (PDB 3C6B) no other cysteines (5 total) were found to be oxidized, similarly in the mass spectra of H160I no other cysteines were found oxidized.

pH Dependence of NEM inhibition of WT SFGH

To probe the effect of substrate on the pK_a of Cys-60 we measured the rate of inhibition of the WT SFGH by NEM at varying pH. We hypothesized that the occupancy of the oxyanion hole could make Cys-60 more prone to oxidation as Cys-60 lies near the peptide bond of one of the oxyanion hole residues, Leu-58-NH (Fig. 1A). To determine if oxyanion hole occupancy affected the reactivity of Cys-60 we utilized *N*-ethylmaleimide and measured the rates of NEM inactivation at varying pH values in the presence or absence of substrate to obtain a pK_a of Cys-60 in each case. NEM-modification of Cys-60 is predominantly responsible for the observed loss of activity as a C60A variant was not significantly inhibited by high concentrations of NEM (6.7 and 7.7 mM); the rates of inhibition of the C60A variant were approximately 4–5 times slower than those observed for the WT enzyme (Supplemental Fig. 2).

The pH-dependence of NEM inhibition [19] of WT SFGH carboxylesterase activity revealed a single pK_a in the absence of substrate, presumably of Cys-60 (the only Cys shown to affect esterase activity when modified), pK_a = 8.7 ± 0.1 (Supplemental

Table 2
Steady-state kinetic parameters for SFGH-catalyzed hydrolysis of pNP-acetate or S-lactoylglutathione. Assays were conducted in Sorensen's buffer at pH 7.4, 22 ± 2 °C.

Enzyme	K_m (mM)	k_{cat} (min^{-1})	k_{cat}/K_m (mM^{-1} min^{-1})	Fold change in k_{cat}/K_m
Substrate = p-nitrophenyl acetate				
WT[a]	0.40 ± 0.07	108 ± 7	270 ± 50	10^{0}
C60S[a]	0.19 ± 0.03	92 ± 3	480 ± 80	$10^{+0.2}$
C60A	0.19 ± 0.05	59 ± 3	310 ± 80	$10^{+0.1}$
N64A	0.78 ± 0.08	66 ± 2	85 ± 9	$10^{-0.5}$
H160I	2.5 ± 0.5	51 ± 4	20 ± 4	$10^{-1.1}$
H160I-ox	3.5 ± 0.8	190 ± 20	50 ± 10	$10^{-0.7}$
H160I-ox w/catalase	2.6 ± 0.6	170 ± 10	70 ± 20	$10^{-0.6}$
H160S	0.16 ± 0.05	29 ± 2	170 ± 50	$10^{-0.2}$
Y278F	0.18 ± 0.04	36 ± 2	200 ± 50	$10^{-0.1}$
W197I[a]	0.054 ± 0.006	63 ± 2	1200 ± 100	$10^{+0.6}$
W197I/C60S[a]	0.14 ± 0.01	45.8 ± 0.7	330 ± 20	$10^{+0.1}$
W197I/H160I	0.99 ± 0.09	2.9 ± 0.1	3.0 ± 0.3	$10^{-2.0}$
Substrate = S-lactoylglutathione				
WT[a]	>1.25			
W197I[a]	3 ± 1	7000 ± 2000	2000 ± 1000	10^{0}
W197I/C60S[a]	3 ± 2	3000 ± 1000	1000 ± 700	$10^{-0.3}$
W197I/H160I	0.9 ± 0.3	7.1 ± 0.8	8 ± 2	$10^{-2.4}$

[a] Data taken from Legler et al. [2].

Fig. 3). Inhibition in the presence of 5 mM pNP-acetate gave a bell-shaped curve and a slightly lower, but not significantly different, pK_{a1} = 8.3 ± 0.3. The descending limb (pK_{a2} = 9.1 ± 0.4) may reflect modification of the enzyme at non-cysteine residues such as histidine [20,21]. The small difference in pK_a values of the ascending limb in the presence or absence of substrate suggests that occupancy of the oxyanion hole has a minor effect (0.4 pH-unit shift) on the pK_a of Cys-60 consistent with increased reactivity with peroxide in the presence of substrate (uncompetitive behavior).

Steady state kinetic parameters of the H160I variant

His-160 is conserved and is found in both SFGH and in *Bacillus subtilis* RsbQ (His-95) (Fig. 1B). The imidazole rings of His-160 and His-276 of the catalytic triad are 3.8 Å from one another (Fig. 1A). To determine if His-160 of SFGH is involved in the oxidative inactivation of SFGH we cloned and expressed an H160I variant. Isoleucine was chosen because it cannot function as a proton or hydrogen bond donor or acceptor. Mutation of His-160 to isoleucine leads to a roughly 6-fold increase in the K_m of pNPA, a 2-fold decrease in the k_{cat} (Table 2) and a $10^{1.1}$-fold decrease in the k_{cat}/K_m suggesting a minor role in substrate binding.

Thermal denaturation of the H160I variant monitored by CD revealed a 7.4 degree decrease in the measured T_m when compared to WT (Table 5). Examination of the structure shows that the His-160 Nε2 is within hydrogen bonding distance (2.8 Å) to the back bone carbonyl of His-276 of the catalytic triad, loss of this hydrogen bond may in part account for the decrease in T_m. His-160 packs with His-276 and the two side chains are found in an eclipsed conformation. His-160 is also within hydrogen bonding distance of a water molecule (WAT-61, Fig. 1A). An analogous water can be found in the structures of RsbQ (WAT-46), Kex1ΔP (WAT-752), and HPP (WAT-22), however, the water which is 6.0 Å from His-276 of the triad is too distant to function as the hydrolytic water in the reaction.

Activation of H160I by peroxide

In the WT enzyme, oxidation of the cysteine results in the inactivation of the esterase. Unexpectedly, mutation of His-160 to Ile, led to the opposite effect, i.e. activation of the esterase upon oxidation of Cys-60 (Fig. 2D). In the absence of substrate, pNPA, the rate of activation by peroxide of the H160I variant was 7-fold faster than the rate of inactivation of WT SFGH suggesting increased reactivity or accessibility of Cys-60 to peroxide.

To determine if the His-160 acted as a proton donor/acceptor or as a hydrogen bond donor/acceptor an H160S variant was made. Mutation of His-160 to serine (H160S), led to peroxide inactivation (Table 3 and Fig. 2E) indicating that His-160 acts only as a hydrogen bond donor in peroxide inactivation.

Steady state kinetic parameters of the H160I variant after treatment with peroxide

To understand how oxidation of Cys-60 affects substrate binding and catalysis the enzyme was treated with pNP-acetate for 1 min followed by peroxide. The treated enzyme was subjected to gel filtration and then assayed with the pNP-acetate substrate immediately following elution. The K_m of the peroxide-treated enzyme (K_m = 3.5 ± 0.8 mM) was comparable to the untreated enzyme (K_m = 2.5 ± 0.5 mM). The addition of catalase had no effect on either the V_{max} (4.9 ± 0.4 U/mg) or K_m (K_m = 2.6 ± 0.6 mM) of the peroxide-treated enzyme after gel filtration indicating that peroxide was not acting as a nucleophile and could not account for the observed increase in the V_{max}. The lack of a significant change in the K_m of the substrate after oxidation of the cysteine suggests that the oxygen(s) (Cys-SOH, Cys-SO_2 and Cys-SO_3) do not significantly block or interfere with pNP-acetate binding in the H160I variant. Only the k_{cat} had increased by 3.7-fold after treatment with peroxide ($V_{max}^{untreated}$ = 1.5 ± 0.1 U/mg; $V_{max}^{treated}$ = 5.5 ± 0.5 U/mg) suggesting that the oxidized cysteine may affect product release and/or catalysis.

Structure of the H160I variant

A structure of the H160I variant was determined by molecular replacement. The structure superposed with the WT SFGH with an rmsd of 0.27 over 269 Cα indicating that the structures are nearly identical. No significant differences in the active site residues were observed when compared to WT (Supplemental Fig. 4 and Supplemental Table 2).

Steady state kinetic parameters of the H160I/W197I double mutant

To examine the role of H160 in the hydrolysis of a glutathione substrate, the H160I/W197I double mutant was used for steady state kinetic analysis of the *S*-lactoylglutathione (SLG) substrate.

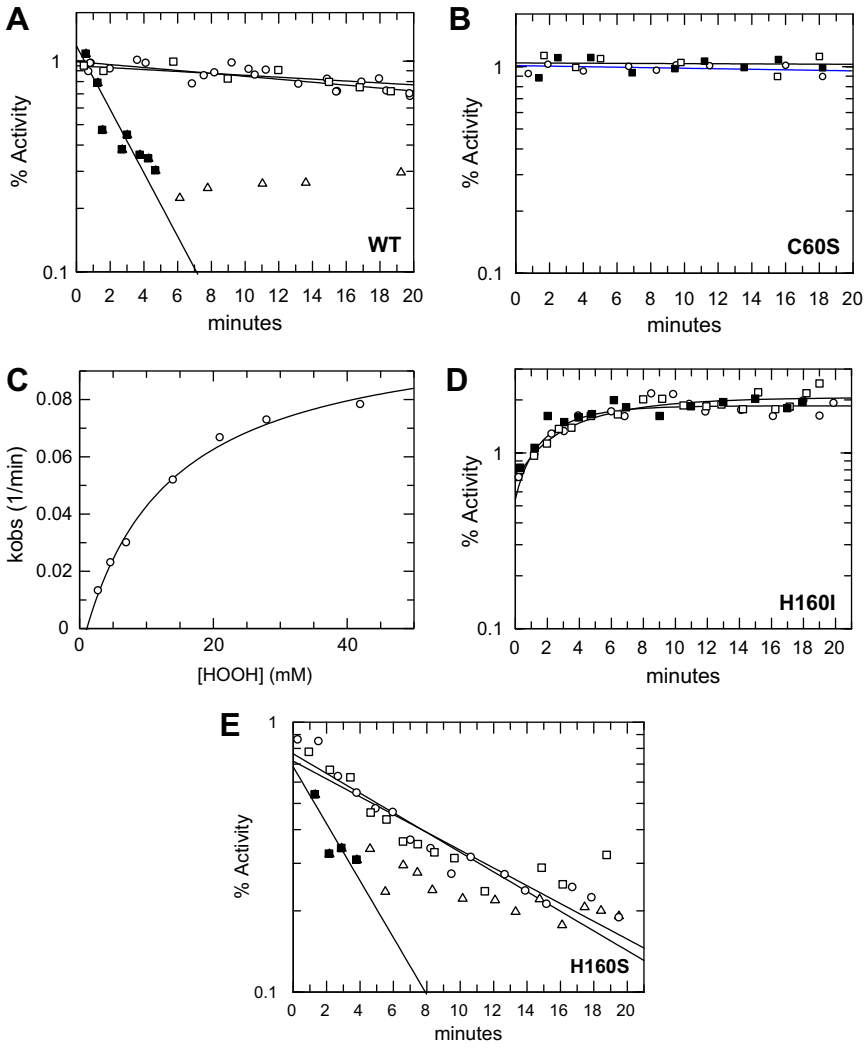

Fig. 2. Inactivation of WT SFGH and the C60S, H160I and H160S variants by peroxide at room temperature (22 °C). (A) Rates of inactivation of WT SFGH by 3.6 mM peroxide measured in the absence of substrate (○), in the presence 5 mM *p*-nitrophenyl acetate (■ and Δ), and in the presence of 5 mM *p*-nitrophenol (□). (B) Rates of inactivation of the C60S variant by 3.6 mM peroxide in the absence of substrate (○), in the presence of 5 mM *p*-nitrophenylacetate (■), and in the presence of 5 mM *p*-nitrophenol (□). (C) The maximum rate of inactivation of WT SFGH and the K_i of peroxide was determined in 1× Sorensen's buffer, pH 7.4 in the absence of substrate. (D) Rates of inactivation of the H160I variant by 3.6 mM peroxide in the absence of substrate (○), in the presence of 5 mM *p*-nitrophenylacetate (■) and in the presence of 5 mM *p*-nitrophenol (□). (E) Rates of inactivation of the H160S variant by peroxide in the absence of substrate (○), in the presence of *p*-nitrophenylacetate (■) and in the presence of 5 mM *p*-nitrophenol (□).

Table 3
Effect of peroxide on SFGH activity in the presence or absence of *p*-nitrophenol (pNP) or *p*-nitrophenyl acetate (pNPA) at room temperature (22 °C) in 1× Sorensen pH 7.4 buffer containing catalase. Graphs are shown in Fig. 2.

Enzyme	pNPA	pNP	[HOOH] (mM)	k_{obs} (1/min)		Rate enhancement with substrate
				Inactivation	Activation	
WT	5 mM	—	3.6	0.29 ± 0.06		26-fold
WT	—	5 mM	3.6	0.010 ± 0.002		
WT	—	—	3.6	0.011 ± 0.002		
C60S	5 mM	—	3.6	0.003 ± 0.003		3-fold
C60S	—	5 mM	3.6	0.001 ± 0.002		
C60S	—	—	3.6	⩽0.002		
H160I	5 mM	—	3.6		0.4 ± 0.1	⩽2-fold
H160I	—	5 mM	3.6		0.21 ± 0.07	
H160I	—	—	3.6		0.4 ± 0.1	
H160S	5 mM	—	3.6	0.2 ± 0.1		2-fold
H160S	—	5 mM	3.6	0.08 ± 0.01		
H160S	—	—	3.6	0.097 ± 0.008		

The H160I/W197I double mutant showed a large $10^{-2.4}$ decrease in k_{cat}/K_m and a minor 3-fold decrease in the K_m of the SLG substrate (Table 2). Similarly with the pNP-acetate substrate a 20-fold increase in the K_m was observed, and a similar $10^{-2.6}$-fold decrease

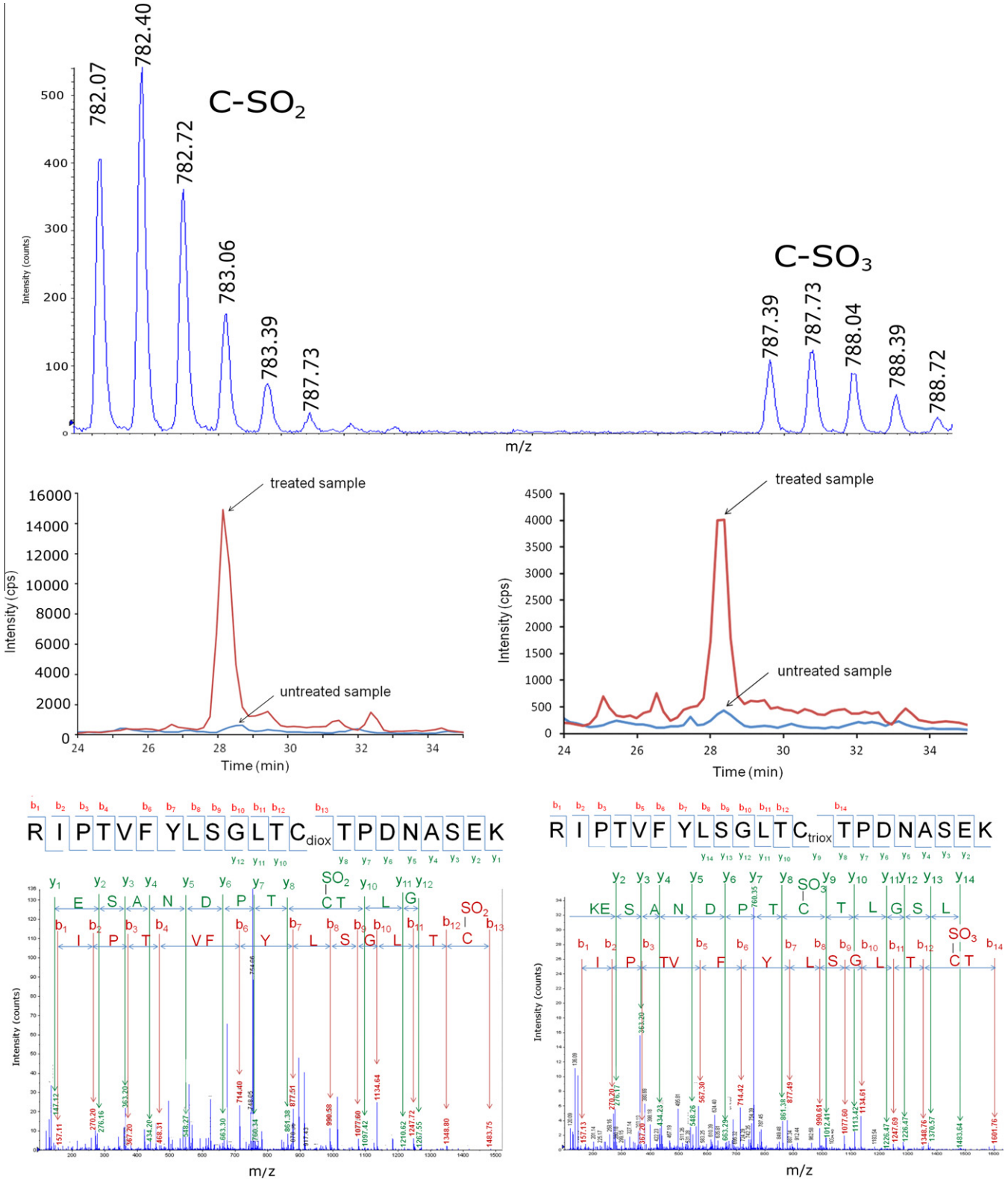

Fig. 3. Tandem electrospray mass spectra of the oxidized H160I variant. (A) Masses of the oxidized peptides containing cysteine sulfinic and sulfonic acids. (B) nanoLC elution profiles of the selected peptides of the treated and untreated samples. (C) Annotated MS/MS spectra of the peptides.

in the k_{cat}/K_m was observed. Thus His-160 does not play a significant role in binding the glutathione substrate, but appears to play a role in binding the pNP-acetate substrate. Based upon the effects on k_{cat}/K_m and k_{cat}, His-160 appears to play an important role in catalysis and/or product release [6].

Steady state kinetic parameters of the Y278F variant

In the structure of the Paraoxon-inhibited SFGH (PDB 3C6B) a short hydrogen bond between Tyr-278-OH and WAT-61 (2.3 Å, Fig. 1A) is found. To determine if the hydrogen bonding interaction

Table 4
Effects of peroxide on the rate constants of activation or inactivation and dissociation constants for peroxide. For the WT enzyme rates were measured at different time points in the presence or absence of catalase to verify that the peroxide in the enzyme solution did not interfere with the measured rate and dissociation constants.

Enzyme	Substrate	k_2 (1/min)[a]	k_{2a} (1/min)	K_i (mM)	K_a (mM)[b]	Catalase
		Inactivation	Activation	Inactivation	Activation	
WT	–	0.116 ± 0.005	–	12 ± 3	–	+
WT	–	0.07 ± 0.02	–	9 ± 4	–	–
WT	5 mM pNPA	1.0 ± 0.5	–	8 ± 5	–	–
H160I	–	–	0.7 ± 0.3	–	5 ± 2	–
H160I	5 mM pNPA	–	1.5 ± 0.4	–	5 ± 4	–
Y278F	–	0.16 ± 0.06	–	10 ± 4	–	–
Y278F	5 mM pNPA	0.3 ± 0.3	–	10 ± 10	–	–

[a] k_2 and k_{2a} are the first order rate constants (inactivation and activation, respectively) for the conversion of the reversible E·HOOH complex to the covalent adduct [11,40].
[b] K_a and K_i are the dissociation constants for initial reversible complex (E + HOOH $\Longleftrightarrow$ E·HOOH).

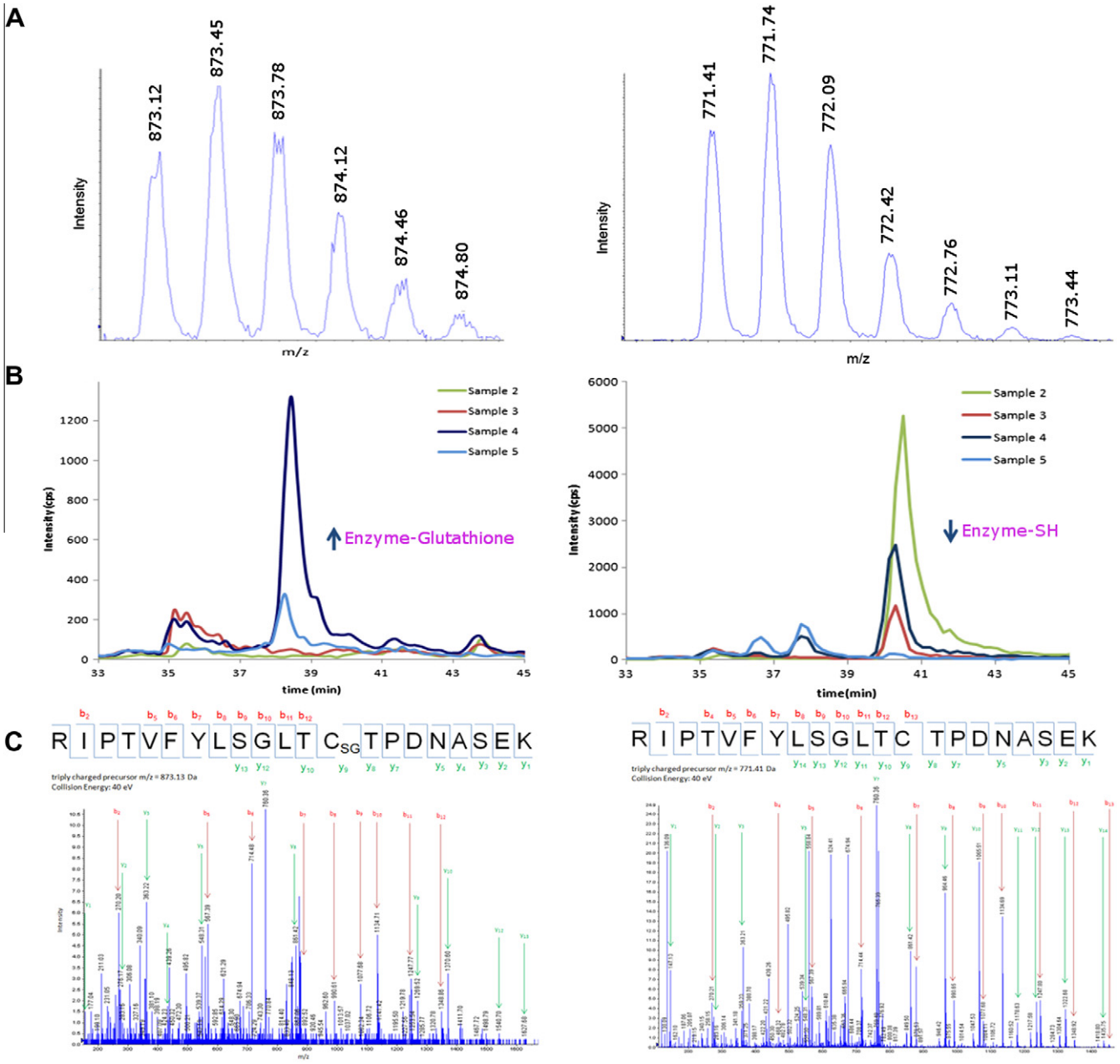

Fig. 4. Observation of the glutathionylated Cys-60 in the presence of pNP-acetate, peroxide and reduced glutathione. (A) Parent ions of the glutathionylated peptide containing Cys-60 (left) and the unmodified Cys-60-SH peptide (right). (B) Comparison of the elution profiles of the parent ions in the enzyme and pNPacetate reaction (sample 2), enzyme, pNPacetate and peroxide (sample 3), enzyme, pNPacetate, peroxide and reduced glutathione (sample 4), and enzyme, pNPacetate, peroxide, and oxidized glutathione (sample 5). (C) Annotated MS/MS spectra of the glutathionylated and reduced peptides.

Table 5
Melting temperatures measured by monitoring the CD signal at 222 nm.

Enzyme	T_m (°C)
WT[a]	69.0 ± 0.1
H160I	61.6 ± 0.1
H160S	58.1 ± 0.2
Y278F	60.6 ± 0.1
W197I[a]	70.6 ± 0.1
W197I/C60S[a]	69.0 ± 0.1
W197I/H160I	64.4 ± 0.2

[a] This data has been taken from [2].

to WAT-61 is important in positioning His-160 and His-276 to facilitate efficient catalysis Tyr-278 was mutated to a Phe. The Y278F variant showed a minor 3-fold reduction in k_{cat}. The K_m of the Y278F variant was not significantly different from that of WT (Table 2).

Structure of the copper coordinated SFGH W197I variant containing a Cys-SO_2

A characteristic feature of D-type serine hydrolase enzymes is their susceptibility to inhibition by Hg^{2+} and Cu^{2+} [1,22–24], two metal ions which can coordinate thiols. To determine if copper coordination of Cys-60 also leads to inhibition we used molecular replacement and site-directed mutagenesis to identify residues involved in copper binding and inhibition. Crystal dimensions, space group and refinement statistics are shown in Supplemental Table 2. After soaking SFGH crystals in paraoxon and copper additional positive difference density at the N-terminus (Fig. 5) and at Cys-60 (Supplemental Fig. 5) was found in the Fo–Fc maps. A copper ion coordinated by the Met-1 carbonyl oxygen, WAT-253 and His-140 Nδ1 could be found in both monomers of the dimer (Fig. 5 B). Bond distances between Met-1 and the copper ion were between 2.2 and 2.5 Å consistent with metal coordination. The metal ion density could be refined (without negative difference density) to an occupancy of 40%. The distance between the copper ion and the nucleophilic serine is ~30 Å, thus, a role in inhibition is unclear. Additional density around Cys-60 could be refined as a cysteine-sulfinic acid (Supplemental Fig. 5). This indicated that copper coordination of Cys-60 could not prevent oxidation of the cysteine. Density for the side chain of His-276 of the catalytic triad was not observed near Ser-161. Instead partial density was observed for a rotamer of His-276 (Supplemental Fig. 5) that was pointed away from the nucleophilic Ser-161. In this conformation, His-276 is unable to participate in catalysis.

Inhibition of WT SFGH and its variants by copper (II) chloride

While copper coordination of Cys-60 was anticipated, it was not observed in the crystal structure. Instead, oxidation of Cys-60 to the sulfinic acid was observed. We hypothesized that copper coordination by Cys-60 in solution was responsible for copper inhibition of D-type esterases. All D-type serine esterases are characterized by their susceptibility to inhibition by Hg and Cu. To determine if Cys-60 was involved in metal ion inhibition (in solution) we analyzed copper inhibition of WT SFGH and its variants and measured initial velocities (~60 s exposure to copper). Cu^{2+} was found to act as a weak non-competitive inhibitor of WT SFGH with a K_i = 18 ± 1 μM (Table 6, Figs. 5 and 6). Non-competitive inhibition is a mixture of both competitive (slope effects due to I binding to free enzyme) and uncompetitive (intercept effects due to I binding to ES) inhibition [25]. Secondary plots of the slope or intercept versus the concentration of copper chloride yielded the dissociation constants K_{is} and K_{ii}, respectively. K_{ii} is the dissociation constant of I from the ESI complex and K_{is} is the dissociation constant of I from EI complex. For complete inhibition, the relationship between the slope or intercept is linear. Non-linear inhibition (parabolic) indicates that there are two molecules of inhibitor binding to one molecule of enzyme (Fig. 6A, inset) [25]. In WT SFGH the concentration of copper needed to double the intercept (K_{ii} = 14 ± 1 μM) is lower than the concentration of copper needed to double the slope (K_{is} = 22 ± 3 μM), indicating two titratable metal ion binding sites. The simplest explanation for our data is that one site affects the slope (competitive), and the other affects the intercept (uncompetitive). Non-competitive inhibition was also observed for the H160I variant, however the sub-plots of the slope and intercept yielded parabolic curves indicating that two molecules of inhibitor could bind a single molecule of enzyme.

Copper (II) chloride also weakly inhibited the C60S and C60A variants. The C60S variant has a K_i (Table 6) comparable to WT SFGH, however further inspection of the slope and intercept effects (Fig. 6B and C, inset) shows a loss of one of the two titratable metal ion sites. Mutation of Cys-60 to either alanine or serine led to uncompetitive inhibition (copper no longer binds the free enzyme). This suggests that Cys-60 is involved in the competitive inhibitor binding site. Uncompetitive inhibition by copper chloride was also observed in the Y278F variant. In the absence of the hydroxyl group of Y278 the effect on the slope is lost and only a parabolic effect on the intercept is observed for this variant, also consistent with the loss of the metal binding site responsible for competitive inhibition.

Copper binds and inhibits at two distinct sites, one site involves Cys-60 and Tyr-278 (competitive inhibitor binding site), consistent with our hypothesis. The second site (uncompetitive inhibitor binding site) may correspond to the N-terminal metal ion binding site identified in the crystal structure (Fig. 5A).

Discussion

The oxidation of cysteines to the sulfenic acid has been proposed to play an important role in redox signaling during oxidative stress [26], however their instability has resulted in a limited number of solved structures containing this oxidized form of cysteine (27 reported). With limited structural information, the assignment of a general motif (either structural or sequence) has been difficult [27]. Here we show that a Dali structural similarity search has uncovered four other enzymes with similar active sites (Fig. 1). One of the identified esterases, RsbQ, is a stress response regulatory protein of the sigma b transcription factor [28]. The active sites of SFGH and of *B. subtilis* RsbQ (1WOM) [28] are the most similar (Fig. 1); each contains a cysteine adjacent to the catalytic triad and a conserved histidine in the $n-1$ position relative to the active site serine. The GXSXG motif for the active site serine is more specifically GHSVG in RsbQ and G^{160}HSMG in SFGH. His-160 is conserved in all known SFGH [6] and plays a role in oxidative inhibition.

Proposed mechanism of oxidative inactivation of WT SFGH and activation of H160I

In the crystal structure of diethylphosphate-inhibited SFGH a water molecule (labeled as WAT-61 in Fig. 1A) can be found within hydrogen bonding distance to Tyr-278, His-160, and the backbone NH of Gly-57. In four of the five structures shown in Fig. 1 a water molecule can be found within hydrogen bonding distance of the $n-1$ residue relative to the nucleophilic serine (histidine, glutamate or tyrosine). The distance between the water and the Oγ of

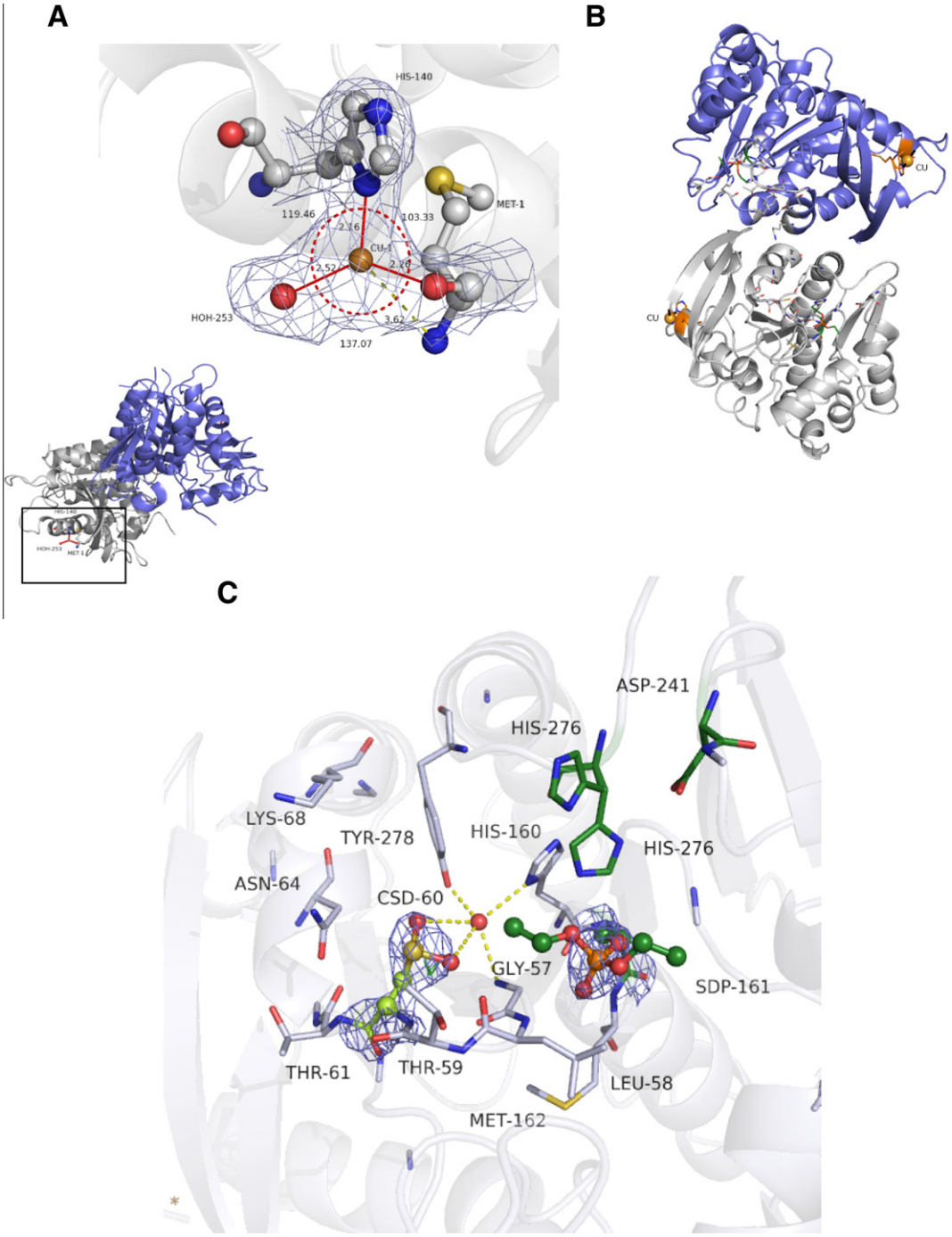

Fig. 5. Structure of the W197I variant inhibited by Paraoxon and $CuCl_2$. (A) Copper binding site at the N-terminus involving His-140 and Met-1. (B) Copper binding sites at the N-termini in the SFGH dimer. (C) Electron density at Cys-60 in the Paraoxon-inhibited W197I variant soaked with $CuCl_2$ was best modeled as a sulfinic acid. Density for the His-276 side chain was not observed for the conformer pointed towards Ser-161.

the nucleophilic serine is 7.0 Å, and is therefore too far to be the water used in the hydrolysis reaction. However, the hydrogen bonding to this water directs the His-160 side chain towards Cys-60. Structurally, no change in the conformation of His-160 was observed when Cys-60 was oxidized to a sulfenic (PDB 3C6B) or sulfinic acid (PDB 4FLM).

The R-SO_3 and R-SO_2 species were observed in mass spectra (Fig. 3) indicating that subsequent rounds of oxidation can occur. The R-SO_2 form was the predominant species in the spectra. Additionally, a plateau was observed in the plots of initial velocity vs. time for the WT and H160I variant (Fig. 2A and D) after treatment with peroxide indicating that a stably oxidized species was responsible for inhibition or activation. In the oxidative inhibition reaction His-160 must function as a hydrogen bond donor or acceptor, but not as a proton donor or acceptor, as the H160S variant was inhibited by peroxide. Examination of the crystal structure of the W197I/DEP variant shows that the His-160 side chain is within hydrogen bonding distance to the aforementioned water and to the backbone carbonyl oxygen of His-276 of the triad. In the structure of the H160I variant, the water is present and no change in the density of the side-chain of His-276 was observed. However, in the structure of the WT enzyme inhibited with copper which contains a

Table 6
Inhibition of WT SFGH and its C60A, C60S, N64A, H160I and Y278F variants by copper chloride. Assays were run in 50 mM Hepes pH 7.0, 150 mM NaCl at room temperature using pNP-acetate as the substrate. K_{is} and K_{ii} were determined from the *x*-intercept in the sub-plots of slope or intercept vs. [I], respectively.

Enzyme	K_i (μM)	K_{ii} (μM)	K_{is} (μM)	Mode of inhibition
WT	18 ± 1	14 ± 1	22 ± 3	Linear non-competitive
C60A	24 ± 3	I-Parabolic		Uncompetitive
C60S	20 ± 2	I-Parabolic		Uncompetitive
N64A	11 ± 3	I-Parabolic	S-Parabolic	Non-competitive
H160I	9 ± 1	I-Parabolic	S-Parabolic	Non-competitive
Y278F	2.1 ± 0.5	I-Parabolic		Uncompetitive

Cys60-SO_2^- density for the His-276 side chain of the catalytic triad was absent in the active site. The side-chain could be modeled in two conformations without the appearance of negative or positive density. The conformer of His-276 which is flipped away from the active site in the Cys-SO_2^- state cannot function in catalysis and may account for the observed inhibitory effect of peroxide.

The activation of the H160I variant by peroxide therefore could be due to the development or utilization of a stronger nucleophile such as peroxide in the esterase reaction. However, enhanced activity was observed even after removal of peroxide by gel filtration and catalase indicating that peroxide did not function as a nucleophile (Table 2). After oxidation, the K_m was not significantly different from that of the untreated H160I. Only, the k_{cat} had increased 3- to 4-fold indicating that product release was faster in the oxidized enzyme. The H160I variant, unlike the WT or H160S variants, must therefore be able to maintain a productive conformation of His-276 in catalysis when the variant is oxidized. The enhancement of k_{cat} could also be due to destabilization of the transition state as the Cys-SO_2 is 3.2 Å from the Gly-57/Leu-58 peptide bond; the Leu-58-NH forms part of the oxyanion hole.

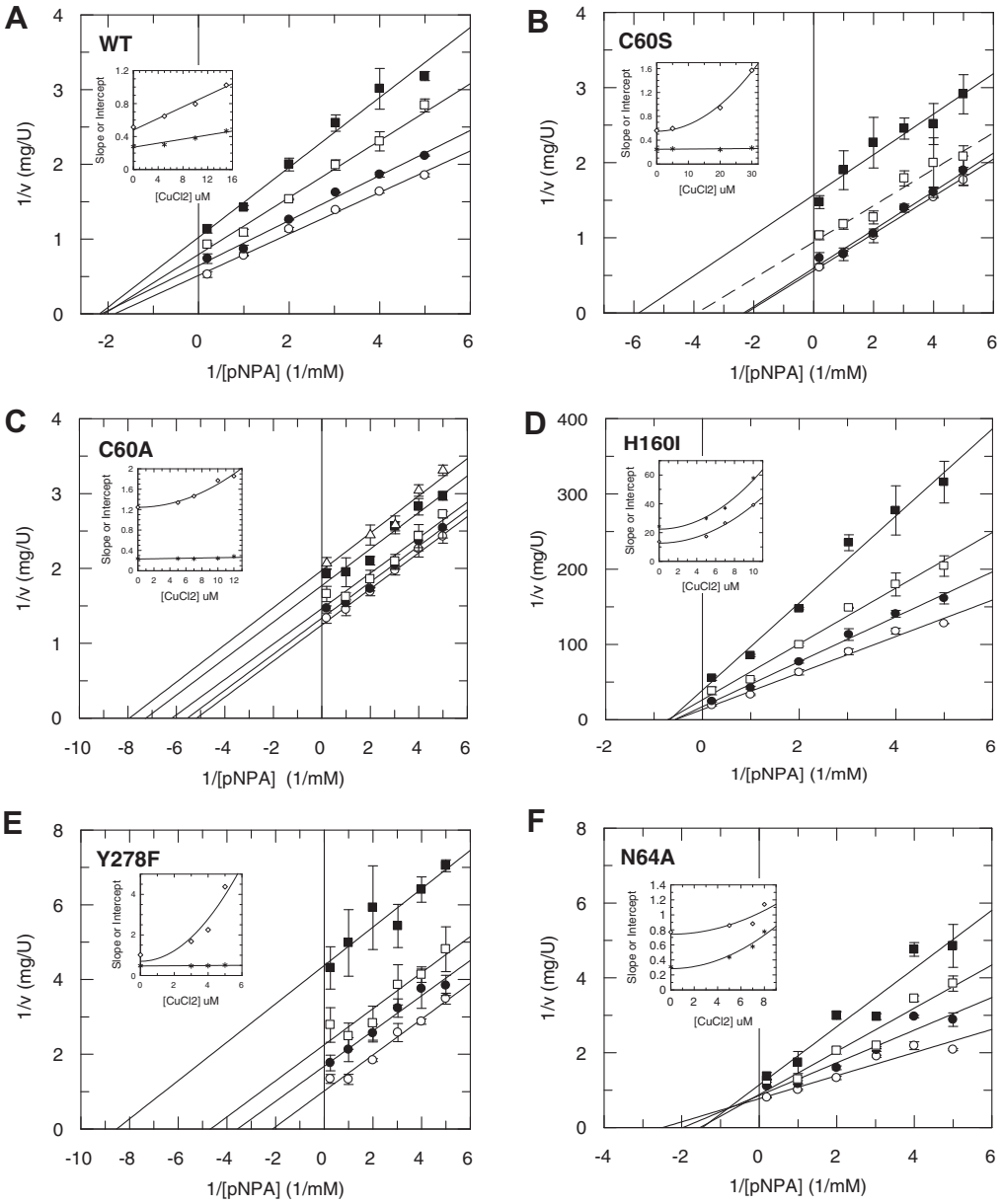

Fig. 6. Inhibition of WT SFGH and its C60S, C60A, H160I, Y278F and N64A variants by copper chloride. All assays were done at room temperature in the presence of 50 mM Hepes pH 7.0, 150 mM NaCl. In the subplots the slope (∗) and intercept (◇) are plotted versus inhibitor concentration. (A) Non-competitive inhibition of the WT enzyme is observed with copper chloride. (B) Uncompetitive inhibition is observed with the C60S variant. (C) Uncompetitive inhibition of the C60A variant. (D) Non-competitive inhibition is observed with the H160I variant. (E) Uncompetitive inhibition of the Y278F variant with copper chloride. (F) Competitive inhibition of N64A variant with copper chloride.

The faster rate of oxidative inhibition of SFGH in the presence of substrate suggested uncompetitive behavior and that, during the esterase reaction, peroxide reacts more quickly with the ES complex, the tetrahedral transition states, and/or acyl-enzyme intermediate than with the free enzyme alone. The dissociation constant of the inhibitor, K_i, is not significantly affected by the presence of substrate, which suggested that a change in the pK_a of the cysteine upon substrate binding or during catalysis may occur. Occupancy of the oxyanion hole with the substrate or transition state of the esterase reaction could favor the deprotonation of Cys-60 (lower the pK_a) if it is connected to the oxyanion hole. We postulated that a decrease in the pK_a of Cys-60 upon substrate binding could account for the increased susceptibility of Cys-60 to oxidation because of the close proximity of Cys-60 to the Leu-58-NH, but found only a small change (0.4 pH unit) in the pK_a of Cys-60 that did not account for the 10-fold increase in the rate of inhibition by peroxide in the presence of substrate. Ferrer-Sueta et al. [29] have made similar observations in peroxiredoxins and concluded that a decrease in the nucleophilic cysteine's pK_a did not generally augment activity. Thus, changes in the pK_a of the cysteine do appear to be as important as originally believed. The uncompetitive behavior was not observed in the H160I or H160S variants. Thus, some other effect (e.g. the binding of the hydrolytic water may enhance the binding of peroxide) must account for the observed uncompetitive behavior.

Other enzymes that contain similar active site configurations: evidence for a oxidation sensitive motif

A Dali structural similarity search identified three serine hydrolases with cysteines adjacent to the peptide bond of the oxyanion hole residue: (1) *B. subtilis* RsbQ (PDB 1WOM), (2) *S. cerevisiae* killer factor and prohormone-processing carboxypeptidase, Kex1ΔP (PDB 1AC5), (3) human protective protein (HPP)/Cathepsin A (PDB 1IVY), and (4) a *Clostridium acetobutylicum* Lipase–esterase (PDB 3E0X). All four enzymes were found to have similar active site configurations, but three of the four enzymes had different residues in the $n-1$ position (equivalent to His-160) relative to the nucleophilic serine when compared to SFGH. In Kex1ΔP and HPP the $n-1$ residue is a negatively charged glutamate residue, while in 3E0X the $n-1$ residue is a tyrosine. RsbQ, like SFGH, contains a histidine at the $n-1$ residue.

The formation of sulfenic acids in these other enzymes has not been reported. However, like SFGH the deamidase activity of lysosomal protective protein (mouse) is inhibited by copper and silver as well as NEM [30]. Similarly, Kex1ΔP can be inactivated by $HgCl_2$ [31,32]. However, in the case of HPP and Kex1ΔP, it is not possible to attribute the metal ion inhibition to the cysteine homologous to Cys-60. In these structures, the homologous cysteine is disulfide bonded and may be significantly less susceptible to oxidation by peroxide. Sulfenic acid formation can also be reversed by disulfide bond formation with displacement of water, thus, it would not be expected to be long-lived in Kex1ΔP or HPP. A second cysteine, Cys-386, near the nucleophilic serine may be involved in Hg inhibition of Kex1ΔP as suggested by Slon-Usakiewicz et al. [33] (Fig. 1C and D). Interestingly, murine Cathepsin A has been shown to be activated by glutathione [30]. One of the products of the SFGH reaction is glutathione and glutathione adducts of SFGH have been observed by us (Fig. 4) and by others [6]. Thus, the sulfenic acid may function as an intermediate in glutathione disulfide formation. Thus, the motif found in these enzymes (Fig. 1) may be involved in binding glutathione and/or Cys glutathionylation. The substrate specificity of RsbQ is currently unknown and more information would be needed to draw a general conclusion about the structural motif.

The structure of the *C. acetobutylicum* Lipase–esterase (Fig. 1E) was solved as part of a structural genomics project. Its active site shows some structural similarities with that of SFGH, but its inhibitor and substrate specificities are not known. Because the $n-1$ residue relative to the nucleophilic serine (equivalent to His-160 in SFGH) is replaced by a Tyr, a potential hydrogen bond donor, it is unclear as to whether this esterase can be inhibited by peroxide.

The work of Stadtman and Levine, linked oxidation to aging and disease [34]. Peroxide can be generated by metabolic reactions and by the metal-catalyzed formation of hydroxyl radicals from hydrogen peroxide (Fenton reaction). The structure of the Paraoxon-inhibited W197I variant with copper contained a Cys-SO_2, however no peroxide was added. Additionally, no peroxide was added to obtain the sulfenic acid in 3C6B. This finding suggested that Cys-60 may be readily susceptible to oxidation when the transition state forms. In solution, millimolar concentrations of peroxide were necessary to achieve the fastest rate of inhibition, however low concentrations of peroxide and a slow rate of oxidation may be more relevant in cases of prolonged oxidative stress. Increased SFGH and aldehyde dehydrogenase level have been associated with breast cancer cell malignancy [35,36], however a defined role has not been proposed and the effects of SFGH mutations have not been studied in breast cancer cell lines. Here we showed how a single mutation, H160I, could alter an enzyme's activity (inhibited to activated) in the presence of peroxide. Such mutations may be important in cellular adaption to oxidative stress or resistance to chemotherapies [37], thus we have not been able to rule out a physiologic role for the oxidized cysteine of SFGH.

The proteomic studies of Carroll et al. have identified 189 proteins containing cysteine-sulfenic acids with diverse functions in signal transduction, DNA repair, metabolism, protein synthesis, nuclear transport, vesicle trafficking and redox homeostasis [5]. They also found overlap among enzymes and proteins found in disulfide, *S*-glutathionylation and *S*-nitrosylation proteomes and those containing sulfenic acids. Intracellularly, SFGH of *Candida boidinii* was shown to be peroxisomal [38], thus SFGH may be a representative example of an enzyme whose activity can be affected by cysteine oxidation by either glutathionylation or by the formation of a sulfenic, sulfinic or sulfonic acid. The structurally similar stress response regulator of the sigma b transcription factor, RsbQ, suggests that SFGH is not the only esterase that carries this oxidation sensitive motif. The sigma b transcription factor enables resistance to oxidative stress [39] and is involved in the energy stress response [28]. Thus, the motif described herein may function as an oxidation sensitive switch that can control the activity of the esterase.

Acknowledgments

We thank Derrick J. Robinson and Benjamin V. Clingan for technical assistance. W.J.H. and D.H.L. gratefully acknowledges the support from the National Research Council Research Associates Program of the National Academies of Science. We thank Dr. Albert S. Mildvan for useful discussions and helpful suggestions.

This work was funded by the U.S. Defense Threat Reduction Agency JSTO award 1.D0015_06_WR_C (CBM) and 1.D0006_08_WR_C (C.B.M. and P.M.L.). The opinions or assertions contained herein belong to the authors and are not necessarily the official views of the U.S. Army, U.S. Navy, or the U.S. Department of Defense.

Appendix A. Supplementary data

Supplementary data associated with this article can be found, in the online version, at http://dx.doi.org/10.1016/j.abb.2012.08.001.

References

[1] A.R. Main, Biochem. J. 75 (1960) 188–195.
[2] P.M. Legler, D. Kumaran, S. Swaminathan, F.W. Studier, C.B. Millard, Biochemistry 47 (2008) 9592–9601.

[3] H.R. Ellis, L.B. Poole, Biochemistry 36 (1997) 15013–15018.
[4] L.B. Poole, Measurement of Protein Sulfenic Acid Content, John Wiley & Sons, I, 2003. editor.
[5] S.E. Leonard, K.G. Reddie, K.S. Carroll, ACS Chem. Biol. 4 (2009) 783–799.
[6] I. Cummins, K. McAuley, A. Fordham-Skelton, R. Schwoerer, P.G. Steel, B.G. Davis, R. Edwards, J. Mol. Biol. 359 (2006) 422–432.
[7] M. Gracanin, M.J. Davies, Free Radic. Biol. Med. 42 (2007) 1543–1551.
[8] R.L. van Montfort, M. Congreve, D. Tisi, R. Carr, H. Jhoti, Nature 423 (2003) 773–777.
[9] A. Claiborne, J.I. Yeh, T.C. Mallett, J. Luba, E.J. Crane III, V. Charrier, D. Parsonage, Biochemistry 38 (1999) 15407–15416.
[10] N. Fujiwara, M. Nakano, S. Kato, D. Yoshihara, T. Ookawara, H. Eguchi, N. Taniguchi, K. Suzuki, J. Biol. Chem. 282 (2007) 35933–35944.
[11] R. Kitz, I.B. Wilson, J. Biol. Chem. 237 (1962) 3245–3249.
[12] G.L. Ellman, K.D. Courtney, V. Andres Jr., R.M. Feather-Stone, Biochem. Pharmacol. 7 (1961) 88–95.
[13] P. Onnerfjord, T.F. Heathfield, D. Heinegard, J. Biol. Chem. 279 (2004) 26–33.
[14] W.J. Hervey, M.B. Strader, G.B. Hurst, J. Proteome Res. 6 (2007) 3054–3061.
[15] J. Navaza, Acta Crystallogr. D Biol. Crystallogr. 57 (2001) 1367–1372.
[16] Collaborative Computational Project, N. 4. Acta Crystallogr. D Biol. Crystallogr. 50 (1994) 760–763.
[17] M.D. Winn, M.N. Isupov, G.N. Murshudov, Acta Crystallogr. D Biol. Crystallogr. 57 (2001) 122–133.
[18] P. Emsley, K. Cowtan, Acta Crystallogr. D Biol. Crystallogr. 60 (2004) 2126–2132.
[19] R.A. Bednar, Biochemistry 29 (1990) 3684–3690.
[20] D.G. Smyth, O.O. Blumenfeld, W. Konigsberg, Biochem. J. 91 (1964) 589–595.
[21] E. Hayon, M. Simic, Radiat. Res. 50 (1972) 464–478.
[22] G. Degrassi, L. Uotila, R. Klima, V. Venturi, Appl. Environ. Microbiol. 65 (1999) 3470–3472.
[23] L. Uotila, M. Koivusalo, J. Biol. Chem. 249 (1974) 7664–7672.
[24] L. Uotila, M. Koivusalo, Methods Enzymol. 77 (1981) 320–325.
[25] W.W. Cleland, Biochim. Biophys. Acta 67 (1963) 188–196.
[26] Y.H. Seo, K.S. Carroll, Angew. Chem. Int. Ed. Engl. 50 (2011) 1342–1345.
[27] F.R. Salsbury Jr., S.T. Knutson, L.B. Poole, J.S. Fetrow, Protein Sci. 17 (2008) 299–312.
[28] T. Kaneko, N. Tanaka, T. Kumasaka, Protein Sci. 14 (2005) 558–565.
[29] G. Ferrer-Sueta, B. Manta, H. Botti, R. Radi, M. Trujillo, A. Denicola, Chem. Res. Toxicol. 24 (2011) 434–450.
[30] T. Chikuma, K. Matsumoto, A. Furukawa, N. Nakayama, R. Yajima, T. Kato, Y. Ishii, A. Tanaka, Anal. Biochem. 233 (1996) 36–41.
[31] L. Latchinian-Sadek, D.Y. Thomas, Eur. J. Biochem. 219 (1994) 647–652.
[32] B.H. Shilton, D.Y. Thomas, M. Cygler, Biochemistry 36 (1997) 9002–9012.
[33] J.J. Slon-Usakiewicz, J. Sivaraman, Y. Li, M. Cygler, Y. Konishi, Biochemistry 39 (2000) 2384–2391.
[34] E.R. Stadtman, R.L. Levine, Amino Acids 25 (2003) 207–218.
[35] A.K. Croker, D. Goodale, J. Chu, C. Postenka, B.D. Hedley, D.A. Hess, A.L. Allan, J. Cell Mol. Med. 13 (2009) 2236–2252.
[36] N. Jessani, Y. Liu, M. Humphrey, B.F. Cravatt, Proc. Natl. Acad. Sci. USA 99 (2002) 10335–10340.
[37] C.N. Landen Jr., B. Goodman, A.A. Katre, A.D. Steg, A.M. Nick, R.L. Stone, L.D. Miller, P.V. Mejia, N.B. Jennings, D.M. Gershenson, R.C. Bast Jr., R.L. Coleman, G. Lopez-Berestein, A.K. Sood, Mol. Cancer Ther. 9 (2010) 3186–3199.
[38] H. Yurimoto, B. Lee, T. Yano, Y. Sakai, N. Kato, Microbiology 149 (2003) 1971–1979.
[39] S. Engelmann, M. Hecker, FEMS Microbiol. Lett. 145 (1996) 63–69.
[40] W.N. Aldridge, Biochem. J. 46 (1950) 451–460.